Asian Journal of Chemistry; Vol. 27, No. 5 (2015), 1626-1630

ASIAN JOURNAL OF CHEMISTRY

http://dx.doi.org/10.14233/ajchem.2015.17421

Fluorescence Studies of Dy^{3+} Ions in Silica Sol Gel

JEENA THOMAS[1], AJITH VERUGHESE GEORGE[1], TIJU J. MATHEW[2] and VINOY THOMAS[2,*]

[1]Department of Chemistry, Mar Ivanios College, Trivandrum-695 015, India
[2]Department of Physics, Christian College, Chengannur-689 122, India

*Corresponding author: E-mail: vinoythoma@gmail.com

Received: 19 February 2014; *Accepted*: 6 May 2014; *Published online*: 20 February 2015; AJC-16856

The fluorescence properties of Dy^{3+} ion are utilized to study the structural changes during the gel to glass transition of the silica xerogels. The fluorescence intensity ratio (yellow to blue, Y/B) is used as a measure of the symmetry of rare earth ion environment during the gel-glass conversion. The high value of the intensity ratio of gel heated to 1000 °C showed that the rare earth ions are embedded in the glassy silica network with an asymmetric environment. Fluorescence study is also used to characterize the effect of metal cation co-dopants on the state of aggregation of rare earth ions in silica sol gel. The addition of co-dopants inhibits the clustering of rare earth ions and promotes better dispersion. The inhibition of clustering is correlated with the generation of strong crystal field bonding sites for rare earth ions in the presence of co-dopants.

Keywords: Rare earth doped materials, Sol gel, Luminescence.

INTRODUCTION

Rare earth doped glasses play an important role for optical applications such as glass lasers and optical fiber amplifiers and also hold promise for photochemical hole-burning memory, flat panel display, *etc*[1]. The potential advantage of the sol-gel method for preparing optical materials includes obtaining new chemical compositions, better purity and more convenient processing conditions[2]. The optical absorption and luminescence properties of several rare earth ions incorporated into sol-gel silica have been reported including Ce(II)[3], Sm(III)[4], Sm(II)[5], Eu(III)[6], Eu(II)[7], Er(III)[8], Tb(III)[9] Yb(III)[10], Pr(III)[11], Dy(III)[12] and Nd(III)[13]. Compact and efficient all solid state lasers emitting in the visible spectral region are of great interest for a number of applications in medicine, biology, metrology, optical storage and display technology. With the ZBLAN material, laser oscillation has been observed in several rare earths such as trivalent praseodymium, neodymium, thulium, holmium and erbium[14]. However, these laser materials do not cover the entire visible spectral range. Gaps especially exist in the yellow and blue range which cannot be filled by applying frequency doubled solid-state lasers. The dopant material dysprosium has the potential to fill these gaps due to the well-known strong fluorescence in the visible spectral range around 575 and 480 nm[15].

In numerous studies on the systems Eu_2O_3-SiO_2, Nd_2O_3-SiO_2, Er_2O_3-SiO_2, Pr_2O_3-SiO_2 and Tb_2O_3-SiO_2 prepared by sol-gel route, it was shown that it is difficult to overcome problem of cluster formation and phase separation[16]. Rare earth clustering has been inhibited by co-doping with Al^{3+} and by using organic acid salts instead of mineral acid salts as rare earth precursors[13]. Jose *et. al.*[16] have shown that the intensity of Eu^{3+} emission in the silica matrix increased remarkably when it is co-doped with CdSe nano crystals. Doped glasses obtained *via* thermal densification of the gels show similar properties with that of the melt route glasses. Thermal treatment of the doped gels changes the local environment of the metal ions, which results changes in fluorescence spectra. Though this behaviour is common for most of the modifier ions doped gels studied, a detailed study of the incorporation of Dy^{3+}ions in silica sol-gel host is limited. In this context, it is interesting to examine the structural evolution and changes in fluorescence properties of Dy^{3+} in the gel to glass conversion. Here we report the results of a study on the luminescence and structural properties of Dy^{3+} doped silica aerogels. The flurescence intensity, full width half maximum and yellow to blue (Y/B) ratio are successfully used to study the asymmetries of the Dy^{3+} sites in glass hosts. We further used the fluorescence spectroscopy to characterize the effect of several cation co-dopant on the fluorescence property of Dy^{3+} in sol-gel derived silica.

EXPERIMENTAL

Silica sols containing 2 equivalent mol % Dy_2O_3 were prepared from tetraethylorthosilicate (TEOS) (Fluka pure

grade), $Dy(NO_3)_3 \cdot 9H_2O$ (Merck, India), doubly distilled deionized water and high purity HNO_3 and NH_4OH. The desired amount of $Cr(NO_3)_3 \cdot 9H_2O$ dissolved in deionized water in the presence of HNO_3 was poured in TEOS under stirring at room temperature. The TEOS/H_2O/HNO_3 molar ratio was 1:14:0.01. The pH of the sols was adjusted to a value of 3 by adding NH_4OH. The sols were cast in petri-dishes. The gels were left for 1 week at room temperature. Transparent crack-free dried monolithic gels were obtained after drying for 14 days in air oven at 60 ± 2 °C. The gels were heated at different temperatures ranging from 200 to 900 °C in a programmable furnace with the rate of 3 °C/h. (The gel with 0.5 mol % became opaque on heat treatment and was not taken for further studies). Transparent crack free and bubble free gels (diameter 20-25 mm, thickness 1.8-2.2 mm) were reproducibly obtained. Optical spectra of the gels and heat treated samples were recorded with a pectrophotofluorimeter (Shimadzu-RFPC 5301). Density of the samples were measured using Archmidie's principle. The co-dopants (10 equivalent mol %) were added in the form of their nitrates. The following equations give the simplified mechanisms leading to the gelation of the precursor solution

$$\equiv Si\text{-}OC_2H_5 + H_2O \rightarrow \equiv Si\text{-}OH + C_2H_5OH \quad (1)$$

$$\equiv Si\text{-}OH + HO\text{-}Si \rightarrow \equiv Si\text{-}O\text{-}Si\equiv + H_2O \quad (2)$$

$$\equiv Si\text{-}OH + H_5C_2O\text{-}Si\equiv \rightarrow \equiv Si\text{-}O\text{-}Si + C_2H_5OH \quad (3)$$

Mechanism (1) represents hydrolysis reaction and mechanisms (2) and (3) represent condensation reactions. Simultaneously a cluster-cluster aggregation process takes place as the sol converts to gel. The rare earth and codopant nitrates become increasingly entangled and ultimately trapped within the growing clusters, which make the dopant ions disperse in the derived gel at a molecular level. All the measurements were made at laboratory temperature.

RESULTS AND DISCUSSION

An important performance indicator for rare earth materials to be useful for glass laser applications is its fluorescence properties. To determine the optical characteristics of the sample photoluminescence measurements were carried out. Fig. 1 shows the excitation spectra for the 575 nm emission of Dy^{3+} doped silica gels heat-treated at various temperatures. The intensity and half bandwidth of the transitions increase with increasing heat treatment temperature. These results have a relation to the environment of Dy^{3+} ions. Because the electrons of the 4*f* shells are screened by the outer shell electrons, the presence of the surrounding lattice has little effect on the *f-f* transitions, the silica network strengthens gradually, $(Si\text{-}O)_n$-Dy bonds form and Dy^{3+} ions are coordinated by SiO_4 tetrahedra instead of H_2O as shown in Fig. 2.

Dy^{3+} ion is situated in a distorted cube with eight non-bridging oxygens belonging to the corners of SiO_4 glass forming tetrahedral, each tetrahedron donating two oxygens.

Fig. 3 shows the emission spectra of the xerogels heat treated at various temperatures. The fluorescence intensity increases remarkably, when the doped silica gel is heat treated in the range 60-1000 °C. The result of the linear shrinkage of the gel *versus* heat treatment temperature shows that the shrinkage at high temperatures is much smaller than that from room

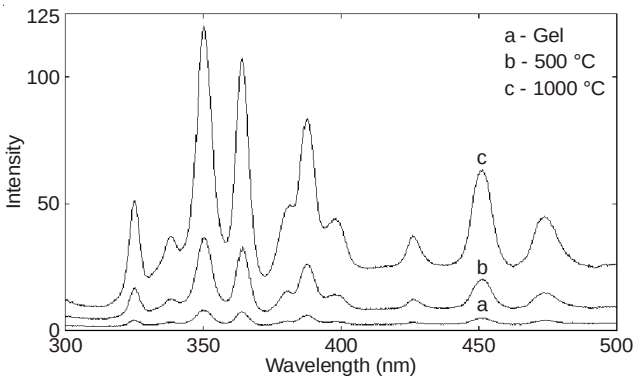

Fig. 1. Excitation spectra of Dy^{3+} in SiO_2 under various heat treatment temperatures

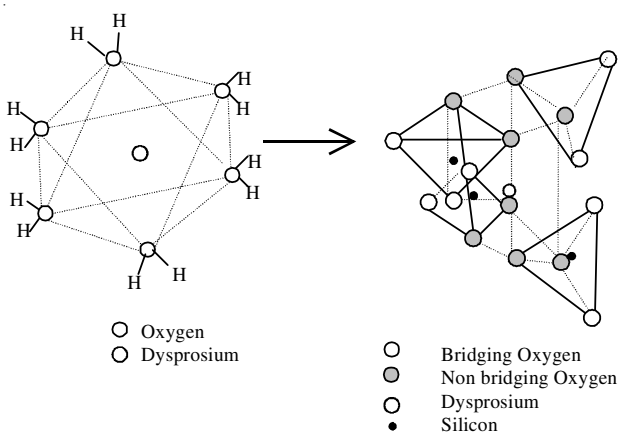

Fig. 2. Structural change of Dy^{3+} during gel to glass transition

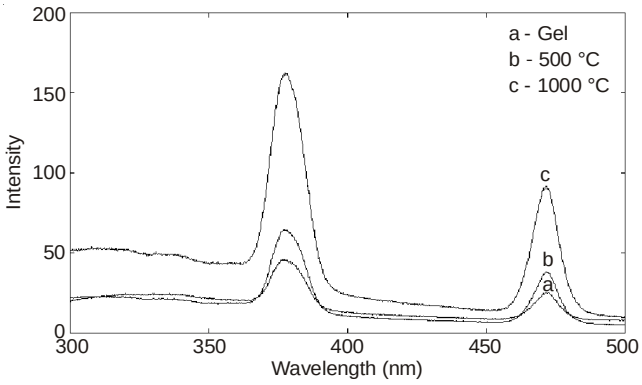

Fig. 3. Emission spectra of Dy^{3+} in silica matrix (λ_{ex} = 355 nm)

temperature to 500 °C. This indicates that the large increase in fluorescence intensity is not caused mainly by the increase in Dy^{3+} ion concentration as a result of the decrease in sample volume[9]. The -OH groups which quench strongly the radiation transitions of Dy^{3+} ion are from the coordination water rather than the physically absorbed water[9]. With increasing heat treatment temperature the silica network strengthens gradually and the coordination water molecules are substituted by SiO_4 tetrahedron. After heating at 600 °C, (Fig. 4) the coordinated water molecules are almost removed by the formation of $(Si\text{-}O)_n$-Dy bonds. The full width half maxima of the emission lines (FWHM) also increase with heat treatment temperature. The variation in FWHM of 470 nm line and 575 nm line are given in Fig. 5. The increase in FWHM confirms the increase in disorder of the local environment of Dy^{3+} ions.

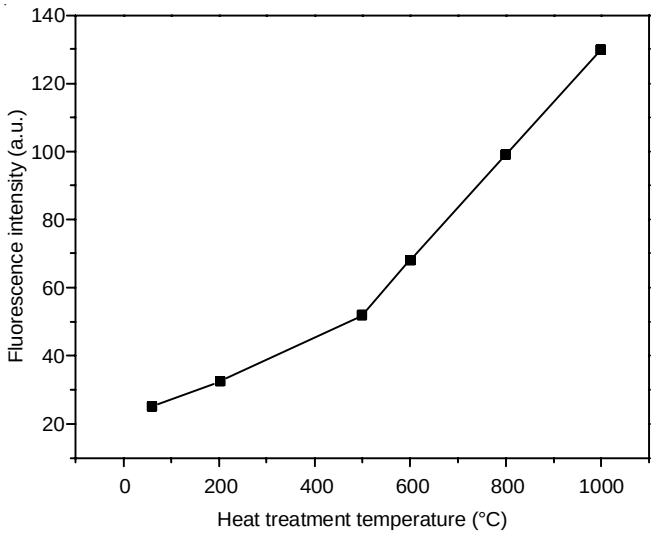

Fig. 4. Increase in fluorescene intensity with heat treatment temperature

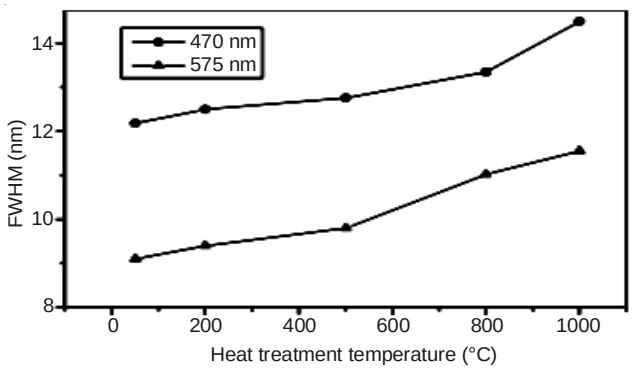

Fig. 5. Variation of full width half maximum (FWHM) with heat tretment temparature

From the emission spectra of Dy^{3+}, the intensity ratio ($^4F_{9/2} \rightarrow {}^6H_{15/2}$)/($^4F_{9/2} \rightarrow {}^6H_{13/2}$) due to emissions in the yellow and blue regions designated as Y/B are calculated. The Y/B of Dy^{3+} emission follows a trend parallel to red to orange (R/O) of Eu^{3+}, as these ratios are influenced by the site symmetry and electronegativity of the ligand atoms in a similar manner. The two prominent transitions are electric dipole in nature out of which ($^4F_{9/2} \rightarrow {}^6H_{13/2}$) is hypersensitive. The intensity of the hypersensitive transition is affected by the metal ligand interactions.

The ratio of their intensities is shown to be sensitive to the covalency of the ligand atoms and distortions from the cubic symmetry[17]. The larger the inequality of the emission intensities of these two transitions, the larger is the asymmetry and covalency effects. For the present case, the Y/B ratio showed a marked increase, as the gel is heat treated (0.51 to 0.76). The high value of the intensity ratio of the 1000 °C heated gel showed that the Dy^{3+} is embedded in the glassy network with an asymmetric environment.

Fig. 6 shows the typical absorption spectra of 2 mol % Dy_2O_3 doped silica gel fired at 900 °C. All the spectra of rare earth ions arise from the intra-configuration transitions within the 4*f* shell. In the free ion state, these transitions are prohibited by the parity rule of electric dipole transition. However this prohibition can be avoided for ions embedded in a crystal field by non-centrally symmetric interactions of the ions with

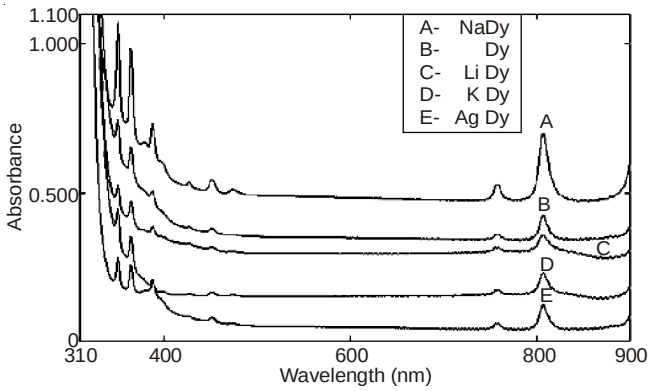

Fig. 6. Optical absorption spectra of Dy^{3+} doped glassy system

surrounding ions, which mix states of opposite parity and thus relax the parity restrictions. For Dy^{3+}ions, the transition occurs from the $^6H_{15/2}$ levels to various excited levels. The experimentally observed absorption spectra of Dy^{3+} ion in the present glassy systems are found to be in good agreement with that of other oxide systems. Owing to the absence of the long-range order in the glass, the micro symmetry around Dy^{3+} ions differs slightly from site to site. Typical half widths of about 200 cm^{-1} for isolated bands. The overall appearance of the spectra does not change very much with glass composition.

Fig. 7 shows that the presence of a cation co-dopant has a strong influence on the fluorescence emission of Dy^{3+} ion. Pure sol-gel silica glass can show a variety of photoluminescence phenomena due to kinds of defects in the sol-/gel silica glass network such as $\equiv Si^*$, $=Si^{**}$, $\equiv Si\text{-}O^*$ and oxygen vacancies, *etc*[18]. As the broad emission band stretching from about 370 to 450 nm in present work is observed in all the samples, it is considered that this band is associated with the defects in the silica sol-gel matrix. Quantitatively the increase in fluorescence intensity varies with the cation co-dopant. The ability of the co-dopant to increase the fluorescence intensity increases as Li > Na > Ag > K. This behaviour can be explained by invoking the influence of the non-radiative rate, hydroxyl quenching and cross-relaxation on the radiative relaxation rate.

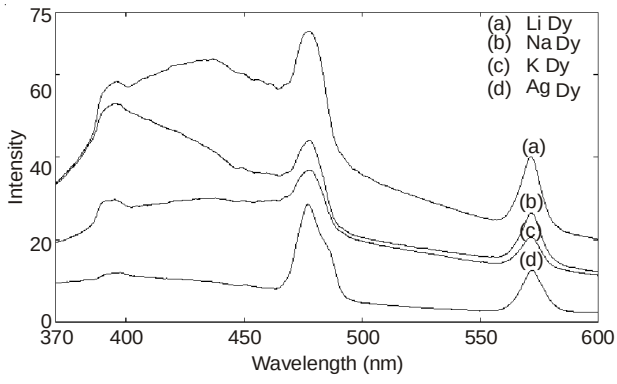

Fig. 7. Emission spectrum of Dy^{3+} in the presence of cations

The total relaxation rate can be expressed as

$$1/\tau = \Sigma W_{NR} + \Sigma A + P_{CR}$$

where ΣA is the total radiative rate, ΣW_{NR} is the non-radiative rate and P_{CR} is the rate of cross-relaxation between adjacent ions.

The possible channels for non-radiative relaxation are discussed below:

(a) Multi-phonon relaxation involving phonons of energy $\hbar\omega$ is described by

$$W_{NR} = A \exp(-Bp)$$

where A and B are constants, p is the number of phonons (excited lattice vibrations) and this can be calculated using the equation

$$p = \frac{\Delta E}{\hbar\omega}$$

where ΔE is the energy gap between emitting and terminal levels. For silica glass the phonon energy is 965 cm^{-1} due to the Si-O-Si stretching vibrationof Q^3 units[19]. In a cation co-doped system the rare earth ions are located in a modified field which has a larger effective mass of the local vibration system than that of purely rare earth doped glass system. This leads to a decrease in phonon energy for the Si-O-Si stretching vibration and the number of phonons needed to bridge the excited and ground state increases[11,20]. With increasing the number of phonons 'p', W_{NR} decreased and as a result the quantum yield increased. Therefore the non-radiative rate is higher in purely rare doped glasses.

(b) The hydroxyl quenching can be described by the relationship

$$\frac{1}{\tau_{em}} = \frac{1}{\tau_{rad}} + k_{OH}\alpha_{OH}$$

where α_{OH} is the absorption coefficient of hydroxyl at 2700 nm (40 cm^{-1}) and k_{OH} is the rate constant. The presence of hydroxyl band will also increase the non-radiative decay. From the FTIR spectra it was confirmed that a large amount of hydroxyl group was present in R doped glasses. The hydroxyl content in glasses processed at high temperature has been estimated from the IR spectra using the relationship

$$[OH](ppm) = (1000/t)\log(T_a/T_b)$$

where T_a and T_b are the transmissions at 2.6 and 2.7 mm, respectively and *t* is the sample thickness (mm). Hydroxyl content around 4000 ppm was measured after the glass processed at 1000 °C. This was explained to be the cause for the greater non-radiative relaxation rate in co-dopant free rare earth doped glasses compared to co-doped glasses.

(c) The cross relaxation may take place between the same lanthanides or between two different ions. This process between a pair of rare earth ions is graphically presented in Fig. 8. When it is excited at 355 nm in high-lying excited states of Dy^{3+} several paths for self quenching by energy transfer between two similar neighboring ions[21]. For example, $[^4F_{9/2}, {}^6H_{15/2}] \rightarrow [^6H_{5/2}, {}^6H_{5/2}]$ or $[^4F_{9/2}, {}^6H_{15/2}] \rightarrow [^6H_{9/2}, {}^6F_{3/2}]$. In the first path, there is a good resonance between the energy of the $^4F_{9/2} \rightarrow {}^6H_{5/2}$ and $^6H_{15/2} \rightarrow {}^6H_{5/2}$ transition. Cross relaxation occurs as follows.

De-excitation of one Dy^{3+} from $^4F_{9/2}$ level to a $^6H_{5/2}$ manifold ($^4F_{9/2} \rightarrow {}^6H_{5/2}$) and energy transfer to another Dy^{3+} ion $^6H_{15/2} \rightarrow {}^6H_{5/2}$ follows by energy dissipation in the silica glass. There are more than six cross-relaxation paths originating from the $^4F_{9/2}$ emitting level and even more when all the excited states are taken into account[19]. By this process the original system loses the energy (E_2-E_1) by obtaining the lower state E_2 (which may also be the ground state E_1) and another system acquires the energy by going to a higher state E_2. The two energy gaps

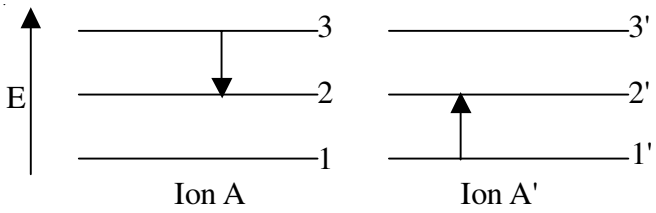

Fig. 8. Schematic diagram of a cross-relaxation process between two ions of the same or different nature

may be equal or can be balanced by one or two phonons. It is a dominating factor at high concentrations. In the present case a small amount of co-dopant prevented the aggregation resulting in the circumvention of the cross relaxation process.

Alumina addition was found to improve the dissolution of rare earths in glasses prepared by vapor phase deposition or melting. Studies indicated that addition of alumina is also effective in dispersing SiO_2 glasses prepared by sol-gel process. It is known that the analysis of the emission properties of rare earth ions can give information on the clustering in glasses. In order to confirm these arguments we have studied the effect of co-dopants on the fluorescence properties of Dy^{3+} ion in SiO_2 matrix. From the fluorescence spectra (Fig. 5) it is clear that the presence of a cation co-dopant has a strong influence on the local bonding environment of the R^{3+}. All the co-dopants lead to the fluorescence enhancement. We attribute the effect to the ability of codopants to penetrate R^{3+} clusters or to inhibit their formation. According to the crystal chemistry approach[22] multiple cation modifiers will co-exist in the modifier rich regions. This implies that when a co-dopant is added to R^{3+} doped sample, it will penetrate the R^{3+} clusters and promote inter dispersion. The inter dispersion occurs because of the formation of R-O-M linkages where M is a co-dopant. The net effect is increased separation and reduced energy transfer between the R^{3+} ions. The field strength of the co-dopant will influence the covalency of the R-O bond[23]. Higher field strength co-dopants in linkages will form stronger, more covalent bonds with oxygen. This in turn leads to weaker, less covalent R-O bonds in the linkage. In effect, there is a competition between R^{3+} and the co-dopant for the electron density associated with oxygen and the higher field strength cation exerts the controlling effect. As a result, the intensity increases remarkably. In either case the average R-R distance increases and as a result the energy transfer decreases thereby increasing the fluorescence intensity.

This observation suggests that the ability of the co-dopants to inhibit R^{3+} clustering decreases as $Li^+ > Na^+ > Ag^+ > K^+$. This ordering is significant because it parallels the trend observed for the field strength (Z/r^2) cation co-dopant (or charge density Z/r) of the cation co-dopant (Table-1). This suggests that high field strength cation co-dopants are more effective at R^{3+} clustering and promoting more uniform distribution of R^{3+} ions than low field strength co-dopants. The comparison with Al^{3+} is complicated by the fact, however that Al^{3+} will act as a network former whereas Li^+, Na^+, K^+ and Ag^+ are expected to act as a network modifiers. It is possible that the charge density effect saturates for modifier and that the network forming capability rather than the charge density governs the effect of Al^{3+} on the clustering of R^{3+}. It is also

TABLE-1
IONIC RADII, CHARGE DENSITIES AND
FIELD STRENGTHS OF THE CODOPANTS

Cation	Ion radius r(Å)	Charge density Z/r ($Å^{-1}$)	Field strength Z/r ($Å^{-2}$)
Li^+	0.68	1.47	2.16
Na^+	0.95	1.05	1.1
K^+	1.33	0.751	0.564
Ag^+	1.26	0.793	0.629

possible that smaller concentrations of high charge density modifiers are as effective at inhibiting R^{3+} clustering as larger concentrations of lower charge density modifiers.

Conclusion

Dy^{3+} doped silica matrices were prepared by sol-gel process and the spectroscopic properties in dried gels and gel glasses were studied. Fluorescence properties were utilized to study the structural changes during the gel to glass transition of the silica xerogels. The increase in the fluorescence intensity ratio and FWHM suggest that the Dy^{3+} ion is embedded in a highly asymmetric environment. The addition of cation codopants promotes the dispersion of rare earth ions. The cation codopants penetrate these clusters and interdisperse with Dy^{3+}. This effect leads to larger Dy^{3+}-Dy^{3+} separations and better isolation of Dy^{3+} ions. This study indicates that the state of aggregation and cross relaxation of rare earth dopant cane be controlled by the addition cation codopants.

ACKNOWLEDGEMENTS

One of the authors (VT) is thankful to University Grants commission (Government of India) for financial assistance.

REFERENCES

1. Y.H. Song, T.Y. Choi, Y.Y. Luo, K. Senthil and D.H. Yoon, *Opt. Mater.*, **33**, 989 (2011).
2. P.I. Paulose, G. Jose, V. Thomas, G. Jose, N.V. Unnikrishnan and M.K.R. Warrier, *Bull. Mater. Sci*., **25**, 69 (2002).
3. A. Patra, D. Kundu and D. Ganguli, *Mater. Lett*., **32**, 43 (1997).
4. N. Danchova and S. Gutzov, *J. Sol. Gel Sci. Technol.*, **66**, 248 (2013).
5. S.T. Selvan, T. Hayakawa and M. Nogami, *J. Phys. Chem. B*, **103**, 7064 (1999).
6. A. Feinle, F. Lavoie-Cardinal, J. Akbarzadeh, H. Peterlik, M. Adlung, C. Wickleder and N. Hüsing, *Chem. Mater*., **24**, 3674 (2012).
7. F. Wu, G. Puc, P. Foy, E. Snitzer and G.H. Sigel Jr., *Mater. Res. Bull*., **28**, 637 (1993).
8. B.T. Stone and K.L. Bray, *J. Non-Cryst. Solids*, **197**, 136 (1996).
9. K. Tonooka and O. Nishimura, *J. Lumin*., **87**, 679 (2000).
10. G. De, A. Licciulli and M. Nacucchi, *J. Non-Cryst. Solids*, **201**, 153 (1996).
11. A. Biswas and H.N. Acharya, *Mater. Res. Bull*., **32**, 1551 (1997).
12. P.V. Jyothy, P.R. Rejikumar, T. Vinoy, S. Kartika and N.V. Unnikrishnan, Pramana, **75**, 999 (2010).
13. S. Chakrabarti, J. Sahu, M. Chakraborty and H.N. Acharya, *J. Non-Cryst. Solids*, **180**, 96 (1994).
14. J.Y. Allain, M. Monerie and H. Poignant, *Electron. Lett*., **26**, 166 (1990).
15. L. Zhang and H. Hu, *J. Phys. Chem. Solids*, **63**, 575 (2002).
16. G. Jose, G. Jose, V. Thomas, C. Joseph, M.A. Ittyachen and N.V. Unnikrishnan, *Mater. Lett*., **57**, 1051 (2003).
17. S. Tanabe, T. Ohyagi, N. Soga and T. Hanada, *Phys. Rev. B*, **46**, 3305 (1992).
18. C.F. Song, M.K. Lü, P. Yang, D. Xu, D.R. Yuan, G.J. Zhou and F. Gu, *Mater. Sci. Eng. B*, **97**, 64 (2003).
19. B. Viana, N. Koslova, P. Aschehoug and C. Sanchez, *J. Mater. Chem*., **5**, 719 (1997).
20. S. Todoroki, S. Tanabe, K. Hirao and N. Soga, *J. Non-Cryst. Solids*, **136**, 213 (1991).
21. N.I. Koslova, B. Viana and C. Sanchez, *J. Mater. Chem*., **3**, 111 (1993).
22. A.J.G. Ellison and P.C. Hess, *J. Non-Cryst. Solids*, **127**, 247 (1991).
23. A.J.G. Ellison and P.C. Hess, *J. Geophys. Res. B*, **95**, 15717 (1990).